Journal of Thermal Analysis and Calorimetry, Vol. 90 (2007) 2, 325–328

GAS VACUOLES FORMATION DURING THE DEHYDRATION OF TREHALOSE DIHYDRATE: A RAMAN MICROSPECTROSCOPY APPROACH

B. Berton[1*], *V. Dupray*[1], *H. Atmani*[1] *and G. Coquerel*[2]

[1]La2B – SMS – UPRES EA 3233 Centre Universitaire d'Evreux – Université de Rouen 1, rue du 7ème Chasseurs – B.P. 281 27002 Evreux cedex, France
[2]UC2M2 – SMS – UPRES EA 3233 – IRCOF – Université de Rouen 1, rue Tesnière, 76821 Mont-Saint-Aignan cedex, France

Dehydration of trehalose dihydrate implemented by slow heating (1 K min^{-1}), has been monitored by Raman microspectroscopy from 25 to 110°C directly on single crystals. Between 90 and 120°C, gas initially trapped in irregular macroscopic defects, reorganizes to form spherical vacuoles. The Raman analysis of these vacuoles highlights that the areas in vicinity of the defects are the first affected by the dehydration mechanisms. Indeed, the progressive amorphization of the crystal starts around these defects.

Keywords: *α-α trehalose, dehydration, gas vacuoles, macroscopic defects, Raman microspectroscopy, single crystals*

Introduction

The α-α trehalose (α-*D*-glucopyranosyl, α-*D*-glucopyranoside) is a non-reducing disaccharide, which contains two *D*-glucose units 1,1 linked by a glycosidic bond ($C_{12}H_{22}O_{11}$–Mw=342.3 g mol^{-1}). This non-toxic sugar is currently used in industry as pharmaceutical excipient [1], food additive [2], and especially as cryoprotectant, for example, for the storage of organs before transplantation [3]. Indeed, the most interesting property of trehalose is its ability to prevent biomaterials from extreme conditions, such as dehydration or freezing. Two hypotheses have been proposed to explain the exceptional bioprotective properties of trehalose: the 'water replacement hypothesis' [4, 5] and the 'vitrification hypothesis' [6]. The first one states that during the drying process, the water molecules are replaced by trehalose molecules that bind to lipids of the biomembrane by hydrogen bonds. 'Vitrification hypothesis' suggests that trehalose can access to a glassy state that forms an amorphous matrix around proteins and membranes. The examination of these hypotheses requires a good knowledge of the trehalose/H_2O binary system.

The dehydration mechanisms of trehalose dihydrate have been the subject of intense research in recent times [7–20]. These studies have reported polymorphic transitions according to various drying process of powders, using mainly differential scanning calorimetry, thermogravimetry or X-ray diffraction. So far, four phases have been clearly identified: a dihydrate T_h (also designated as form I [7]), two anhydrous forms T_β (or form III) and T_α (or form II), and an amorphous material T_r. The dihydrate, T_h is the stable phase at room temperature. The crystallographic structure of this commercial compound is orthorhombic, $P2_12_12_1$ [21]. The anhydrous T_β is a monoclinic, $P2_1$, and is stable at room temperatures [7]. This form can be obtained for example by heating T_h at 130°C during 4 h [14]. The T_α form is an isomorph desolvate of trehalose T_h [14]. It is produced from the dihydrate by a 'smooth' dehydration, for example by vacuum evaporation at 50°C during 48 h [7]. The amorphous T_r is obtained, for example, by melting T_α at 135°C [12]. Various studies have shown that the dehydration mechanism depends on many parameters such as particle size [8–10], heating rate [13, 14, 17, 20], hygrometry [1, 15] or lattice defects [10]. It is important to note that all these studies involved powdered samples that, by nature, present a high degree of polycrystallinity and heterogeneity.

Recently, in order to avoid the effects of this heterogeneity, Mallet *et al.* [22] studied the dehydration mechanisms of trehalose on 'large' single crystals (in the order of several millimetres). During this study using optical thermomicroscopy, they observed the nucleation and growth of vacuoles inside the particles. However, the optical technique used for their observations did not allow the identification of the nature of these vacuoles. The aim of this study is to characterize, by Raman microspectroscopy, the species present in these vacuoles in order to improve the knowledge on the dehydration mechanisms of trehalose.

* Author for correspondence: Benjamin.Berton@univ-rouen.fr

1388–6150/$20.00

Akadémiai Kiadó, Budapest, Hungary
Springer, Dordrecht, The Netherlands

Experimental

Trehalose single crystals

Trehalose dihydrate (T_h) was purchased from ACROS with a purity grade better than 99% and was used without further purification. To obtain large single crystals, a saturated solution (46.6 g T_h/100 g solution) was prepared by dissolving T_h powder in ultra-pure water (resistivity: 18 MΩ cm). The solution has been left for recrystallization by slow evaporation at ambient condition. Single crystals were obtained after several days of evaporation, then stored at room temperature in ambient air.

Trehalose polymorphic forms

In order to determine the composition of the vacuoles, reference Raman spectra of various trehalose phases have been carried out. The various solids were prepared in the following way:

- The β anhydrous form, T_β was obtained according to the procedure of Sussich *et al.* [14] by heating trehalose dihydrate at 130°C for 4 h.
- The α anhydrous form, T_α was obtained by 'smooth' dehydration [14] (i.e. after heating trehalose dihydrate at 50°C in a closed container with desiccant P_2O_5 during 15 h and quenched to room temperature in the container to avoid rehydration).
- The amorphous state, T_r was obtained by melting T_α at 135°C [12].
- Trehalose solution 10% is a solution of trehalose (10 g T_h/100 g solution) prepared by dissolving T_h powder in ultrapure water.

Thermomicroscopy

Samples were heated at 1 K min^{-1} until the appearance of vacuoles with a heating stage LINKAM THMS 600. Samples were placed in a quartz crucible. The dehydration process was then monitored by optical microscopy.

Raman microspectroscopy

Raman measurements were carried out at ambient temperature by using a confocal Raman microscope similar to the system described by Schuster *et al.* [23]. It is composed of a Raman spectrometer (LabRam HR by Jobin-Yvon Horiba with a 600 lines/mm grating) coupled to a microscope (Model BX41, Olympus) with *xyz* mapping stage via optical fibers. The excitation of Raman scattering is operated with a helium–neon laser at a wavelength of 632.8 nm. The laser beam is focused on the crystal by the microscope objective x50LWF. A confocal pinhole of 100 μm diameter in front of the entrance slit rejects Raman signal from out of focus planes. This enables a spatial resolution within the range 1–2 μm that also minimizes the background of the quartz carrier slides. The spectral resolution used is 4 cm^{-1} . Calibration was performed by referring to the 520 cm^{-1} line of silicon. Raman spectra with good signal-to-noise ratios were obtained by using integration times from 30 to 90 s. The investigations of the Raman spectra were carried out at room temperature in the range of 2600–3600 cm^{-1}.

Results and discussion

Reference Raman spectra of the different trehalose forms

Figure 1 shows the expansion of the 2800–3600 cm^{-1} region for the different trehalose forms. Our spectra are in good agreement with those reported in the literature [7, 8]. The region between 2880 and 3100 cm^{-1} has already been correlated to the vibrations arising from the symmetrical and asymmetrical stretching of the ring CH modes [24–27]. However a precise assignment is difficult because the bands are mainly related to coupled modes.

The comparison with the other spectra highlights the existence of specific bands corresponding to each

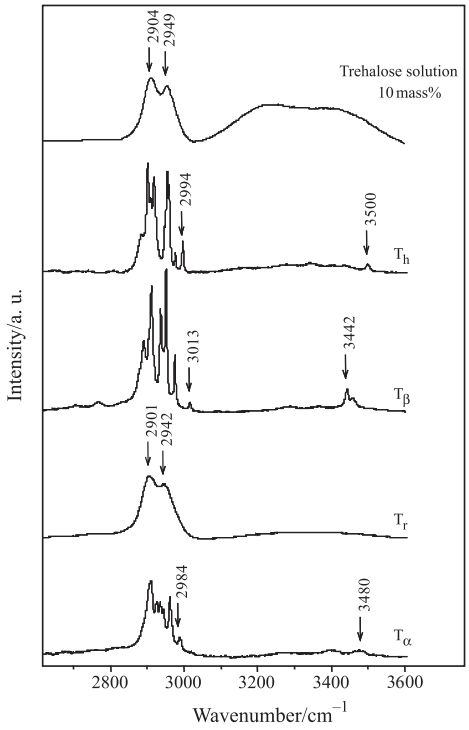

Fig. 1 Raman spectra of different polymorphous forms of trehalose in the 2800–3600 cm^{-1} region

polymorphic form. The following bands can be considered more particularly: 2994 and 3500 cm^{-1} for T_h, 3013 and 3442 cm^{-1} for T_β and 2984 cm^{-1} for T_α. The Raman spectrum of T_r is typical of amorphous materials with a very small number of broad bands. This spectrum is almost similar to the one obtained for a solution of trehalose. The main difference is due to the broad band between 3100 and 3500 cm^{-1} (vibration modes of liquid water) on the solution spectrum. This band is often very small in amorphous trehalose even if it might contain residual water.

Thermomicroscopy and Raman study of dehydration of T_h single crystals

At ambient temperature, single crystals have an isometric habitus. About half of the crystals contain internal macroscopic defects similar to those observed by Mallet *et al.* [22] (Fig. 2a). The Raman spectroscopy study shows that this initial crystal is made of T_h except for the macroscopic irregular defects. Indeed, in these areas, the Raman signal is very weak (20 times lower than the signal measured in the rest of the crystal). One can suppose that these defects contain gas. Some gas initially dissolved in the solution has been trapped inside the particle during the crystal growth.

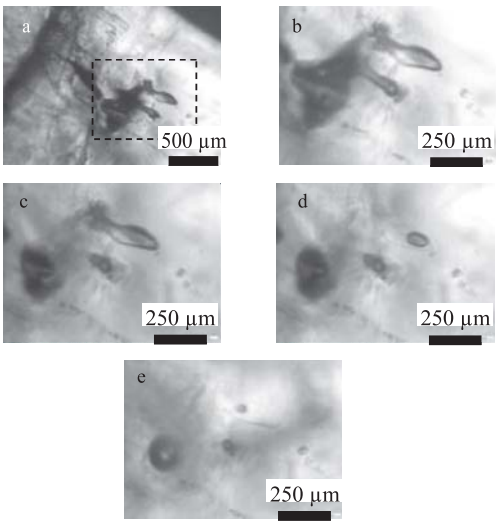

Fig. 2 Optical thermomicroscopy photographs presenting inner macroscopic defects in T_h single crystals at various temperatures (scan rate: 1 K min^{-1}). a – 25, b – 93, c – 96, d – 98, e – 102°C

The thermomicroscopy study of crystal dehydration confirms the formation of vacuoles (Fig. 2b to e). This phenomenon appears systematically in the immediate vicinity of the macroscopic defects, for temperatures ranging from 90 to 102°C. At these temperatures, one can simultaneously observe the progressive disappearance of the defects and the growth of the vacuoles. These vacuoles are stable up to the melting point at 200°C. In case of cooling prior melting these vacuoles remain unchanged for months. The diameter of the vacuoles varies, from one crystal to another, between 10 and 200 µm.

Figure 3a presents the Raman spectroscopy *X–Y* mapping of a crystal heated up to the formation of the vacuoles (102°C) and then cooled down to ambient temperature. This mapping shows the presence of T_h for the major part of the crystal (Fig. 3c). The presence of the peak at 3500 cm^{-1} indicates that there is still some water trapped in the crystal. Two areas present spectra different from those of the remainder of the crystal. A fine layer around the vacuoles (the thickness does not exceeds few micrometers) presents the signal of amorphous trehalose (Fig. 3d). Finally, inside the vacuoles a very weak Raman signal can be observed (Fig. 3b). This result gives evidence of the absence of condensed matter (trehalose or solution) inside this spherical room.

This study shows that most of the single crystals contain gas trapped inside the bulk, forming

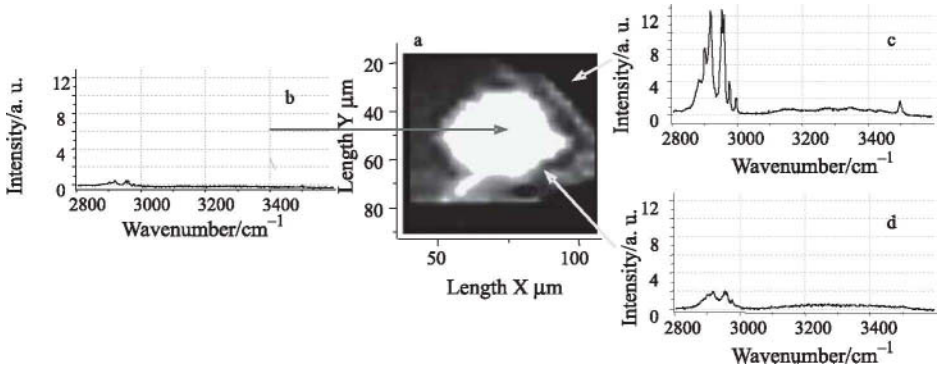

Fig. 3 Two-dimensional Raman investigation of a T_h single crystal heated until formation of the vacuoles (102°C) and then cooled at ambient temperature. a – Raman map of the main peak (2901 cm^{-1}) intensity, the brighter is a point in the maps, the higher is the corresponding Raman intensity, b – Raman signal inside the vacuole, c – Raman signal of the major part of the crystal, d – Raman signal around the vacuole

macroscopic irregular defects. During the heating, the gas reorganizes in the crystals to form spherical bubbles namely the vacuoles. The Raman analysis show that at 102°C the nature of the major part of the crystal did not change, only the trehalose present in the vicinity of the defects changed structure: $T_h \rightarrow T_r$. Moreover the first stage of dehydration can be characterized by an amorphisation of the trehalose [8, 12, 17, 18], then the dehydration process begins on the level of the defects. These results illustrate the high impact of physical parameters on the dehydration pathways. In this study: crystal size, heating rate and macro-crystallinity of the initial particles were fixed, however we observed noticeable heterogeneity in terms of behaviors even inside single crystals. This could, at least partly, explain the numerous dehydration mechanisms of polycrystalline trehalose powders published in the literature.

Conclusions

This study gives evidence of formation of gaseous vacuoles inside trehalose single crystals submitted to a slow heating rate (1 K min^{-1}). Our data show the formation of gas bubbles at the beginning of the dehydration process, between 90 and 102°C. This gas, initially trapped in ill-defined macroscopic defects gathers to form vacuoles. At least locally, this gas influences the dehydration mechanism of trehalose. Indeed, the first transformations ($T_h \rightarrow T_r$) during the dehydration occur near to these defects. Thus any prediction of the dehydration mechanism should take into account more physical parameters than previously thought such as the structural purity [28], and the nature, the concentration and the location of macroscopic defects. Thus, a strict control of both the nucleation and the crystal growth of the trehalose dihydrate T_h are of primary importance to control the dehydration.

Therefore, in order to interpret the exact role of these defects under various conditions of dehydration, supplementary studies are needed on single crystals with various internal qualities, (containing a variable number of macroscopic defects). For example, crystallization processes starting from more or less saturated solutions with various gases can be envisaged.

References

1 M. D. Jone, J. C. Hooton and M. L. Dawson, Int. J. Pharm., 313 (2006) 87.
2 B. Roser, Trends Food Sci. Technol., 2 (1991) 166.
3 A. D. Braz, J. Med. Biol. Res., 28 (1995) 169.
4 J. H. Crowe, L. M. Crowe, J. F. Carpenter and C. A. Wistrom, Biochem. J., 241 (1987) 1.
5 J. H. Crowe, L. M. Crowe, J. F. Carpenter, A. S. Rudolph, C. A. Wistrom, B. J. Spargo and T. J. Anchordoguy, Biochim. Biophys. Acta, 947 (1988) 367.
6 H. Levine and L. Slade, Biopharm., 5 (1992) 36.
7 A. M. Gil, P. S. Belton and V. Felix, Spectrochim. Acta A, 52 (1996) 1649.
8 L. S. Taylor, A. C. Williams and P. York, Pharm. Res., 15 (1998) 1207.
9 L. S. Taylor and P. York, J. Pharm. Sci., 87 (1998) 347.
10 L. S. Taylor and P. York, Int. J. Pharm., 167 (1998) 215.
11 F. Sussich, F. Princivalle and A. Cesàro, Carbohydr. Res., 322 (1999) 113.
12 F. Sussich, C. Skopec, J. Brady and A. Cesàro, Carbohydr. Res., 334 (2001) 165.
13 F. Sussich, S. Bortoluzzi and A. Cesàro, Thermochim. Acta, 391 (2002) 137.
14 H. Nagase, T. Endo, H. Ueda and M. Nagakagi, Carbohydr. Res., 337 (2002) 167.
15 T. Furuki, A. Kishi and M. Sakurai, Carbohydr. Res., 340 (2005) 429.
16 J. F. Willart, F. Danede, A. De Gusseme, M. Descamps and C. Neves, J. Phys. Chem. B, 107 (2003) 11158.
17 J. F. Willart, A. De Gusseme, S. Hemon, M. Descamps, F. Leveiller and A. Rameau, J. Phys. Chem. B, 106 (2002) 3365.
18 K. Akao, Y. Okubo, N. Asakawa, Y. Inoue and M. Sakurai, Carbohydr. Res., 334 (2001) 233.
19 D. Kilburn, S. Townrow, V. Meunier, R. Richardson, A. Alam and J. Ubbink, Nature Materials, 5 (2006) 632.
20 F. Sussich and A. Cesàro, J. Therm. Anal. Cal., 62 (2000) 757.
21 G. M. Brown, D. C. Rohrer, B. Berking, C. A. Beevers, R. O. Gould and R. Simpson, Acta Cryst., B28 (1972) 3258.
22 F. Mallet, S. Petit and G. Coquerel, BIWIC 11 – ISBN 89-89637-23-6, (2004) 190.
23 K. C. Schuster, E. Urlaub and J. R. Gapes, J. Microbiol. Methods, 42 (2000) 29.
24 D. S. Carr and B. L. Harris, Ind. Eng. Chem., 41 (1949) 2014.
25 K. De Gussem, P. Vandenabeele, A. Verbeken and L. Moens, Spectrochim. Acta A, 61 (2004) 2896.
26 K. Akao, Y. Okubo, N. Asakawa, Y. Inoue and M. Sakurai, Carbohydr. Res., 334 (2001) 233.
27 F. S. Paarker, Application of Infrared, Raman and Resonance Raman Spectroscopy in Biochemistry, Plenum Press, New York, London 1983.
28 G. Coquerel, Chem. Eng. Proc., 45 (2006) 857.

DOI: 10.1007/s10973-007-8384-1